*The Korean Journal of Ceramics*, **6**[2] 138-142 (2000)

# Effect of RTA Treatment on $LiNbO_3$ MFS Memory Capacitors

**Seok-Won Choi, Yu-Shin Choi, Dong-Gun Lim, Sang-Il Moon, Sung-Hoon Kim, Bum-Sik Jang and Junsin Yi**

*Department of Electrical Engineering, Sungkyunkwan Univ.*
*300 Chunchun-Dong, Jangan-Gu, Suwon, Kyunggi-Do, 440-746 Korea*
(Received September 23, 1998)

Thin film $LiNbO_3$ MFS (metal-ferroelectric-semiconductor) capacitor showed improved characteristics such as low interface trap density, low interaction with Si substrate, and large remanent polarization. This paper reports ferroelectric $LiNbO_3$ thin films grown directly on p-type Si (100) substrates by 13.56 MHz RF magnetron sputtering system for FRAM (ferroelectric random access memory) applications. RTA (rapid thermal anneal) treatment was performed for as-deposited films in an oxygen atmosphere at 600°C for 60 sec. We learned from X-ray diffraction that the RTA treated films were changed from amorphous to poly-crystalline $LiNbO_3$ which exhibited (012), (015), (022), and (023) plane. Low temperature film growth and post RTA treatments improved the leakage current of $LiNbO_3$ films while keeping other properties almost as same as high substrate temperature grown samples. The leakage current density of $LiNbO_3$ films decreased from $10^{-5}$ to $10^{-7}$ A/cm$^2$ after RTA treatment. Breakdown electric field of the films exhibited higher than 500 kV/cm. C-V curves showed the clockwise hysteresis which represents ferroelectric switching characteristics. Calculated dielectric constant of thin film $LiNbO_3$ illustrated as high as 27.9. From ferroelectric measurement, the remanent polarization and coercive field were achieved as 1.37 μC/cm$^2$ and 170 kV/cm, respectively.

***Key words:*** MFS capacitor, Ferroelectric, $LiNbO_3$, Remanent polarization, RTA

## I. Introduction

FRAMs (ferroelectric random access memories) are considered to be ideal memory devices, which have nonvolatility and high speed read/write characteristics. In particular, MFSFETs (metal-ferroelectric-semiconductor FETs) find applications in intelligent memory devices and functional neuron devices.[1] The MFSFET permits non-destructive read/out characteristics while other FRAM allows only destructive read/out mode. Conventional ferroelectric materials such as $Pb(Zr_xTi_{1-x})O_3$, $BaTiO_3$, and $(Ba_xSr_{1-x})TiO_3$ have been investigated for the development of Gigabit scale dynamic random access memory (DRAM) and destructive read/out mode nonvolatile memory applications.[2-4] These materials are adopted in MIM (metal-insulator-metal) type memory storage because of the prior mentioned materials are strongly interact with Si surface. To circumvent this interdiffusion problem, several researchers investigated materials such as $Bi_4Ti_3O_{12}$, $LiNbO_3$, and $BaMgF_4$ that may generate good interface characteristics at a process temperature over 700°C. Unique combination of optical and electrical properties of $LiNbO_3$[5] demonstrated optoelectronic sensors with a proper ferroelectric nature for a MFSFET device. $LiNbO_3$ transistor showed relatively stable characteristics, low interface trap densities, and large remanent polarizations.[6,7] To manufacture the MFSFETs, it is highly important to establish the physical properties of MFS capacitors. However, conventional ferroelectric films exhibited problems on the Si interface because of high temperature process. To overcome the problems, we selected $LiNbO_3$ and employed low thermal budget process. This paper describes the electrical properties of $LiNbO_3$ thin films deposited at a relatively low temperature below 300°C. The $Ar/O_2$ gas ratio was controlled very carefully in order to obtain stoichiometric $LiNbO_3$ films. Using RTA, we improved the electrical properties of $LiNbO_3$ thin films.

## II. Experiment

Fig. 1 shows an experimental procedure of this work to see

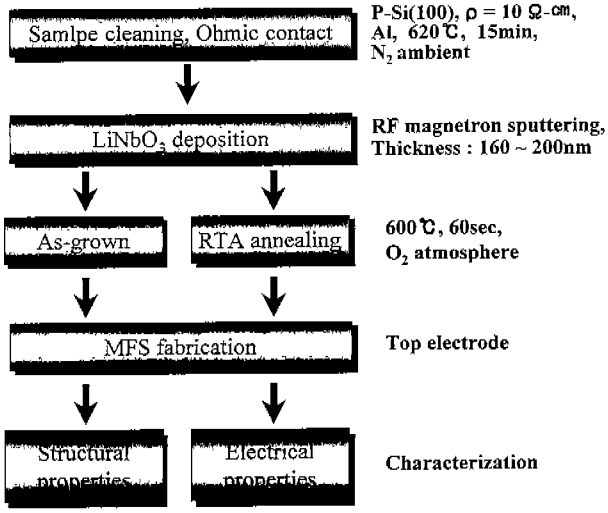


**Fig. 1.** Employed experimental procedure of this paper to investigate the effects of RTA treatment on $LiNbO_3$ MFS capacitors.

the effects of RTA treatment on $LiNbO_3$ MFS capacitors. P-type Si (100) substrates were cleaned in acetone, methanol, and deionized water. To remove substrate contamination, p-type Si substrate was cleaned by RCA method. Backside ohmic contact was formed by thick Al deposition and thermal treatment at 620°C for 15 min. During the back side contact treatment, a nitrogen dominating environment was created by suppling $N_2$ gas at a rate of 2.5 lpm to prevent oxidation. To remove thin oxide layer that may have formed during backside contact treatment, front surface of Si was dipped to BHF (49% HF : $H_2O$=1 : 10) for few seconds. We created base pressure of low $10^{-6}$ torr prior to the $LiNbO_3$ thin film growth. The films were grown by 13.56 MHz RF magnetron sputtering system using a ceramic target ($Nb_2O_5/Li_2CO_3$=51.4/48.6) of 2 inch diameter. Because high temperature processes have to be avoided to prevent degradation of the interface ($LiNbO_3$/Si), we deposited $LiNbO_3$ films at 300°C. The $Ar/O_2$ gas ratio needs to be controlled very carefully in order to obtain stoichiometric $LiNbO_3$ films. In our experiment, the $Ar/O_2$ gas ratio was changed between 6/4 and 9/1. To make a ferroelectric phase transition of $LiNbO_3$ film, as-deposited films were subjected to RTA treatments in an oxygen ambient at 600°C for 60 sec. Aluminum metal was evaporated to define a capacitor area and to measure the electrical properties. The crystallinities of $LiNbO_3$ thin films were investigated by X-ray diffractormeter of Mac Science M18XHF-SRA. Leakage cur-rent density was measured using a Keithley 617 multimeter and Fluke 5100B voltage source. Capacitance-voltage characteristics were measured using a Boonton 7200 C-V meter at 1 MHz. For the ferroelectric properties, P-E loops of $LiNbO_3$ thin films were examined by RT66A in Sawyer-Tower circuit mode. Ferroelectric properties such as coercive field and remanent polarization were obtained by the analysis of P-E loops.

## III. Results and Discussions

Four points probe resistivity measurement on (100) p-type Si substrate exhibited the resistivity of 10~15 Ω-cm. Fig. 2 shows current density versus electric field characteristics of MFS capacitor in reverse bias mode. The I-V characteristics of $LiNbO_3$ films before and after anneal treatment exhibited that RTA treatments could contribute to improve the leakage current of $LiNbO_3$ MFS capacitor. In high field region, the leakage current density was improved by about 2 orders. The decreased leakage current after RTA treatment thought to be resulted from the reduction of oxygen deficiencies and the formation of thin $SiO_2$ layer at the interface.[8] At a fixed electric field of 500 kV/cm, the resistivity of the ferroelectric $LiNbO_3$ film was increased from $2\times10^{10}$ Ω-cm for an as-grown film to $1\times10^{12}$ Ω-cm after 600°C RTA treatment. Fig. 3 shows the leakage current density of annealed $LiNbO_3$ thin films at the various $Ar/(Ar+O_2)$ gas ratio. The low leakage current is observed for the films deposited in 40% oxygen partial pressure, which may be due to formation of highly resistive film with decreased oxygen deficiencies. Breakdown electric field of the films exhibited higher than 500 kV/cm.

Fig. 4 shows the capacitance-voltage characteristics of $LiNbO_3$ films. The C-V curves showed the clockwise hysteresis representing ferroelectric switching characteristics of MFS capacitor. The clockwise hysteresis means that ferroelectric hysteresis controls the Si surface potential and suggests this could be applied to MFSFET memory devices.[9] The C-V curve of the as-grown $LiNbO_3$ thin films show a negative shift and distorted shape. This shift indicates the effect of interface trapped charge, which means the donor-like states distributed at the interface of $LiNbO_3$ and p-type Si substrate. It seems that these charge states are caused by the damaged surface states during the $LiNbO_3$ film deposition. This shift was decreased by curing unstable interface

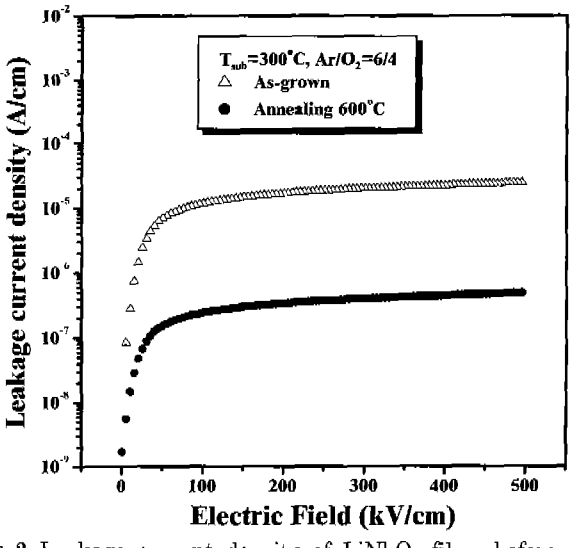


**Fig. 2.** Leakage current density of $LiNbO_3$ films before and after RTA treatment.

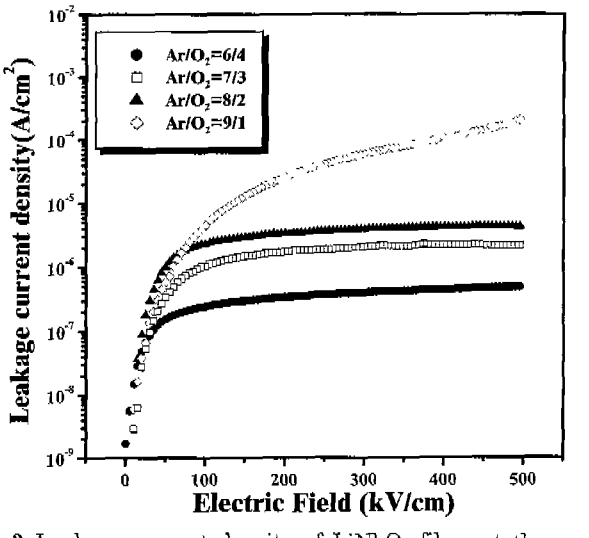


**Fig. 3.** Leakage current density of $LiNbO_3$ films at the various $Ar/O_2$ gas ratio.

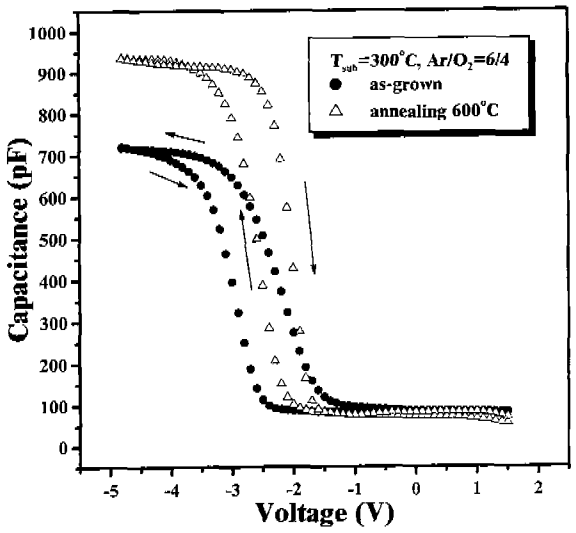


**Fig. 4.** C-V characteristics of $LiNbO_3$ thin films before and after RTA treatment.

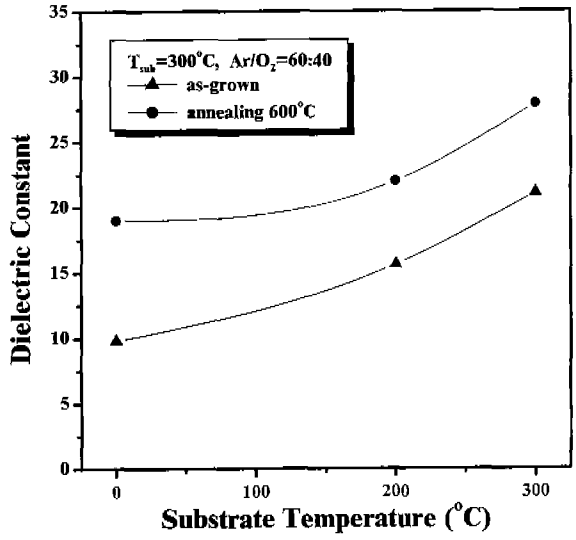


**Fig. 5.** The dielectric constants of $LiNbO_3$ thin films before and after RTA treatment.

states using the post anneal treatment. After annealing, a negative shift was decreased greatly. Fig. 5 illustrates the variation of the effective dielectric constant before and after RTA anneal treatment for the films deposited at a substrate temperature below 300°C. The dielectric constants are increased with the elevation of a film growth temperature. The films after RTA treatment exhibited higher dielectric constant than that of as-grown sample due to increased grain size and improved film crystallinity. The dielectric constant showed a maximum value for the film deposited at 300°C. The calculated dielectric constant of thin film $LiNbO_3$ indicated as high as 27.9 which approach to the bulk value of 30. The possible reasons for a small deviation of dielectric constant in comparison to the bulk $LiNbO_3$ can be explained by the imperfect film crystal structure and the existence of unexpected $SiO_2$ layer at the interface between

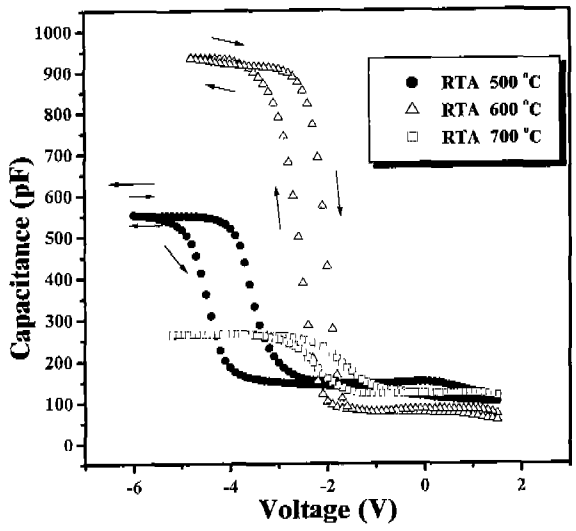


**Fig. 6.** C-V characteristics of $LiNbO_3$ thin films at the various RTA temperatures.

$LiNbO_3$ and Si substrate.[10]

Fig. 6 shows the C-V curves of $LiNbO_3$ films with various RTA temperatures. For the sample treated at 500°C RTA, we observed counter clockwise hysteresis in C-V curves. This result suggest that RTA anneal treatment of 500°C is not enough to use $LiNbO_3$ films in FRAM application. As RTA temperature reached to 600°C, the $LiNbO_3$ film capacitors demonstrated higher capacitance value and clockwise hysteresis. Further increase of RTA temperature to 700°C resulted in degradation of C-V properties while keeping clockwise hysteresis. $LiNbO_3$ film annealed at 700°C may have generated a low dielectric constant materials because Li out-diffusion promote a formation of non-ferroeletric $Nb_2O_5$ phase. From the investigations of RTA temperature effect, we recommend RTA temperature of 600°C for the future device fabrications. Fig. 7 shows the C-V curves of

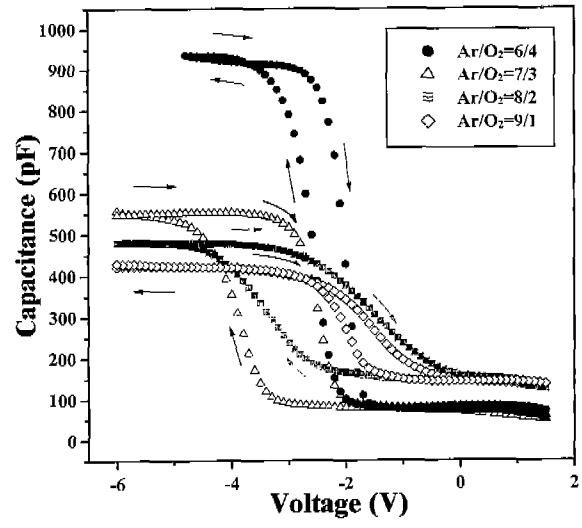


**Fig. 7.** C-V characteristics of $LiNbO_3$ thin films at the various $Ar/O_2$ gas ratio.

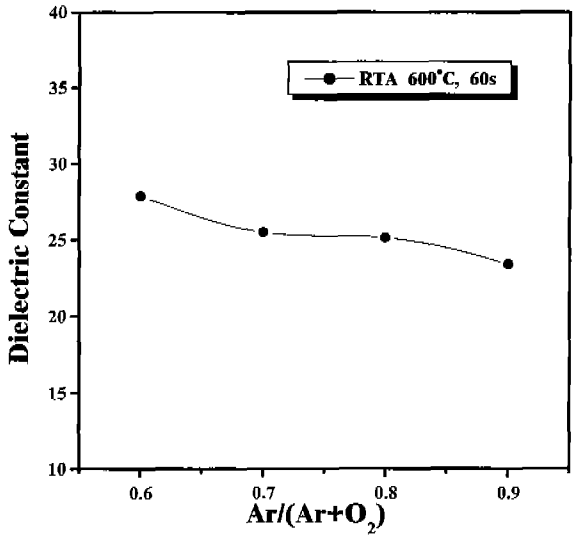


**Fig. 8.** The dielectric constants of $LiNbO_3$ thin films at the various $Ar/O_2$ gas ratio.

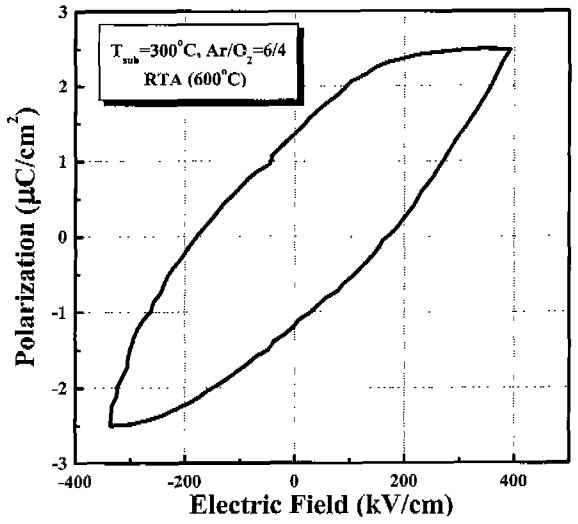


**Fig. 10.** P-E hysteresis loop characteristics of MFS capacitor.

annealed $LiNbO_3$ films with various $Ar/O_2$ gas ratio. All the C-V curves illustrated the clockwise hysteresis characteristics independent of $Ar/O_2$ gas ratio. However, $Ar/O_2$ gas ratio of 6/4 gave the best C-V result indicating that 40% oxygen partial pressure forms the best stoichiometric $LiNbO_3$ films. Fig. 8 shows the dielectric constants with various $Ar/O_2$ gas ratio. We obtained the highest dielectric constant of $LiNbO_3$ film deposited in 40% oxygen partial pressure because the stoichiometric oxide has a higher dielectric constant than nonstoichiometric oxide.

X-ray diffraction was performed to investigate the crystallinity of $LiNbO_3$ thin films. Fig. 9 shows the X-ray diffraction pattern of the $LiNbO_3$ thin film deposited on p-Si(100). We learned from X-ray diffraction that RTA annealed films were changed from amorphous to poly-crystalline $LiNbO_3$ which exhibited (012), (115), (022) and (023) plane. Improved crystallinity with post-annealing well explains the increased dielectric constant after RTA treatment. Examining XRD patterns of $LiNbO_3$ films, we observed the existence of non-ferroelectric $Nb_2O_5$ phase which is responsible for a decreased remanent polarization. This $Nb_2O_5$ phase was detected almost all deposition conditions and after RTA treatment. We consider this Li deficient phase can be removed by supplying excess Li source during the film growth. The P-E hysteresis loop for an annealed $LiNbO_3$ film is shown in Fig. 10. The remanent polarization Pr and coercive field Ec indicated 1.37 $\mu C/cm^2$ and 170 kV/cm, respectively. The lower value of polarization and higher value of coercive field could be the consequencies of small grain size and the large stress in the film. The decrease of this Pr in comparison to that of the bulk $LiNbO_3$ may be due to the existence of grain boundary defects in the film as well as Li deficiencies.

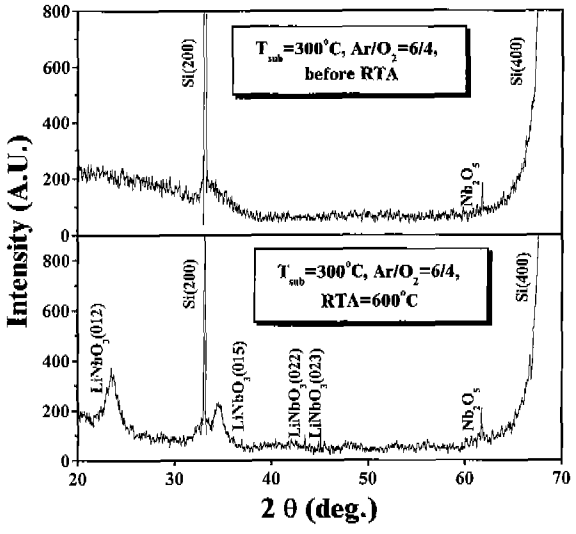


**Fig. 9.** XRD patterns before and after RTA treatment.

## IV. Conclusions

In this paper we established a two-step process to prevent undesired interaction between $LiNbO_3$ film and Si substrate. Using the film grown at a low substrate temperature and subsequent RTA treatment method, this paper demonstrated improved characteristics of electrical and structural properties for $LiNbO_3$ MFS capacitors. after Having 600°C. RTA treatment, the $LiNbO_3$ films exhibited reduced leakage current density by 2 orders and increased resistivity of $1\times10^{12}$ Ω-cm at an electric field of 500 kV/cm. X-ray diffraction indicated that RTA annealed $LiNbO_3$ films were changed from amorphous to poly-crystalline states. The highest dielectric constant of thin film $LiNbO_3$ showed close to that of bulk $LiNbO_3$. The remanent polarization Pr and coercive field $E_c$ were achieved upto 1.37 $\mu C/cm^2$ and 170 kV/cm, respectively. We recommend the growth tempera-

ture of 300°C, $Ar/O_2$ partial pressure of 6/4, and RTA treatment of 600°C, 30 sec. Further studies will be directed to reduce $Nb_2O_5$ by supplying $Li_2O$.

## Acknowledgments

This work was supported by Institute of Information Technology Assessment. Authors recognize IITA for the valuable financial support on this work.

## References

1. M. Shimizu, T. Horiuchi and K. Matsushige, *Jpn. J. Appl. Phys.*, **34**, 5113-5115 (1995).
2. T. Nakmura, *Jpn. Appl. Phys.*, **33**, 5297 (1994).
3. D. J. Eichorst, *Integrated Ferroelectrics*, **4**, 39 (1994).
4. K. Abe, *Jap. J. Appl. Phys.*, **30**(9B), 2152 (1993).
5. H. Ishiwara, *Jpn. J. Appl. Phys.*, **32**, 442 (1993).
6. J. Chen, K. S. Ho and J. Lin, T. A. Rabson, *Intergrated Ferroelectrics*, **10**, 215-222 (1995).
7. C. H. J. Huang and T. A. Rabson, *Integrated Ferroelectrics*, **4**, 293-304 (1994).
8. S. H. Nam and H. G. Kim, *Integrated Ferroelectrics*, **152**, 79-84 (1994).
9. Y. Oishi, Y. Matsumuro and M. Okuyama, *Jpn. J. Appl. Phys.*, **36**, 5896-5899 (1997).
10. W. G. Lee and S. I. Woo, *Integrated Ferroelectrics*, **9**, 21-29 (1995).